Peroxidase Activity of Cationic Metalloporphyrin-Antibody Complexes

Hiroyasu Yamaguchi, Kaori Tsubouchi, Kazuhide Kawaguchi, Eri Horita, and Akira Harada*[a]

Abstract: Peroxidase activity of a complex of water-soluble cationic metalloporphyrin with anti-cationic porphyrin antibody is reported. Antibody 12E11G, which was prepared by immunization with a conjugate of 5-(4-carboxyphenyl)-10,15,20-tris(4-methylpyridyl)porphine iodide (3MPy1C), bound to tetramethylpyridylporphyrin iron complex (Fe^{III}–TMPyP) with the dissociation constant of 2.6×10^{-7} M. The complex of antibody 12E11G with Fe^{III}–TMPyP catalyzed oxidation of pyrogallol, catechol, and guaiacol. A Lineweaver–Burk plot for the oxidation of pyrogallol catalyzed by the Fe^{III}–TMPyP–antibody complex showed $K_m = 8.6$ mM and $k_{cat} = 680\ min^{-1}$. Under the same conditions, K_m and k_{cat} for horseradish peroxidase (HRP) were 0.8 mM and $1750\ min^{-1}$, respectively. Although the binding interaction of the antibody to the substrates was one order lower than that of native HRP, the peroxidase activity of this system was in the same order of magnitude as that of HRP.

Keywords: catalytic antibodies · oxidation · peroxidase · porphyrinoids · pyrogallol

Introduction

It is well known that porphyrins play an important role as functional molecules in a wide variety of biological systems.[1,2] In nature, there are a number of functional molecules that have porphyrin derivatives as cofactors in their active sites or their reaction centers, for example, oxygen carriers such as hemoglobin and myoglobin, redoxidase such as catalase and peroxidase, electron transfer carriers, cytochromes. Special functions of metalloporphyrins in those systems appear in an environment where metalloporphyrin moieties are included in proteins.[3]

A large number of artificial hemoprotein model systems are being developed in an attempt to provide insights for structure-activity relationships, understand the minimal requirements for function, and construct tailor-made molecules.[4] De novo designed hemoproteins have provided keen insight into the fundamental factors which govern the protein secondary and tertiary structural specificity.[5–9] The use of proteins with greater biological homology has facilitated the incorporation of hemes. A rearrangement of the amino acid residues by the site-directed mutagenesis or a chemical modification by the introduction of a functional group at the active residue on the protein surface is also one of the engineering toward functionalization of hemoprotein.[10,11] However, it seems to be difficult to construct an artificial hemoprotein with a novel function by these methods because of the disfavored conformational changes of polypeptides or non-selective reaction of chemicals on the surface of the protein. Recently, reconstruction of hemoprotein has been carried out by introduction of a functionalized metalloporphyrin into naturally occurring hemoproteins to control chemical reactivity or photochemical property.[12–15] However, the use of naturally occurring proteins might be limited due to the decrease of affinity of the proteins for the artificial porphyrins. One of the most convenient methods to incorporate artificial porphyrins into protein matrices is thought to be preparation of monoclonal antibodies for porphyrins.[16–25] The ability of immune system to generate selectively antibodies against virtually any molecule of interest has resulted in the widespread use of antibodies not only as diagnostic agents but also as catalysts in chemical laboratories and industry. Recently Lerner et al. reported that antibodies, regardless of source or antigenic specificity, could generate H_2O_2 from singlet molecular oxygen and this process was catalytic.[26,27] The high durability against H_2O_2 and the ability to generate H_2O_2 of antibodies were considered to be the cause to have a high catalytic activity on the oxidation.

Monoclonal antibodies have become more and more important with high potential as new chemical materials. The development of general strategies for introducing catalytic

[a] Dr. H. Yamaguchi, K. Tsubouchi, K. Kawaguchi, E. Horita, Prof. A. Harada
Department of Macromolecular Science
Graduate School of Science, Osaka University
Toyonaka, Osaka 560-0043 (Japan)
Fax: (+81) 6-6850-5445
E-mail: harada@chem.sci.osaka-u.ac.jp

 DOI: 10.1002/chem.200305692

activity into antigen combining sites of the antibodies should lead to a new class of enzyme-like catalysts with tailored substrate specificities. Strategies that allow incorporation of cofactors such as porphyrins into the binding domain of the antibody should expand the scope of antibody catalysis.[28–31] In nature, it is well known that anionic porphyrin derivatives (di-carboxylic compounds) are used as a cofactor in various functional proteins. However, there are no cationic porphyrins to be seen in a naturally occurring system. Cationic porphyrins such as *meso*-tetrakis-(4-*N*-methylpyridyl)porphyrin (TMPyP) and its related analogues are known to bind DNA as well as cleave DNA.[32] They are known to exhibit a marked anticancer activity with relatively low toxicity and a highly superoxide dismutase (SOD) activity. It is suggested that they may increase the concentration of H_2O_2 in cancer cells.[33–36]

Previously, we prepared monoclonal antibodies against an anionic porphyrin, *meso*-tetrakis(4-carboxyphenyl)porphyrin (TCPP),[19,22,24] and these antibodies have been found to form complexes with metalloporphyrins (metal: Zn, Fe, Mn) specifically. The complexes between anti-TCPP antibody and metalloporphyrins (Fe, Mn) were found to have peroxidase-like activity.[25] In this paper, we have prepared monoclonal antibodies for a cationic porphyrin (5-(4-carboxyphenyl)-10,15,20-tris-(4-methylpyridyl)-porphine iodide (3MPy1C), see below) and investigated the peroxidase-like activity of the complex between the antibody and the corresponding iron porphyrin. The catalytic activity of the antibody–porphyrin complex on the oxidation of pyrogallol was compared with that of horseradish peroxidase (HRP).

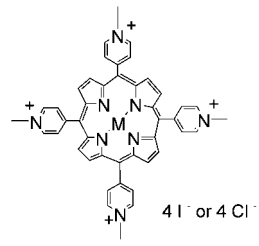

M = 2H: TMPyP
M = Fe-Cl: Fe^{III}-TMPyP

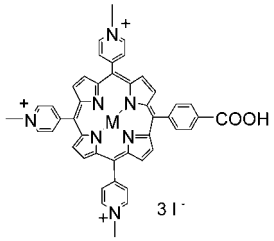

M = 2H: 3MPy1C

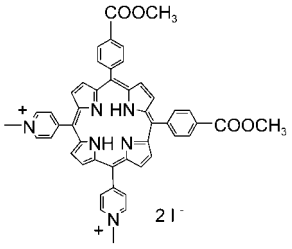

cis-2MPyP

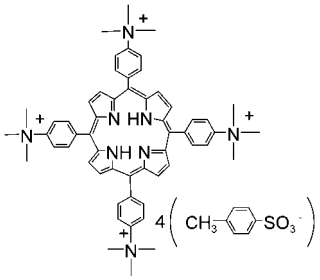

TTMAPP

Results and Discussion

Preparation of monoclonal antibodies against cationic porphyrins: Hapten, 5-(4-carboxyphenyl)-10,15,20-tris-(4-methylpyridyl)-porphine iodide (3MPy1C) was synthesized as shown in Scheme 1. The cationic porphyrin, 3Mpy1C, was coupled to keyhole limpet hemocyanin (KLH) and bovine serum albumin (BSA) via activation of the carboxyl group in the porphyrin molecule using carbonyldiimidazole (CDI). The conjugates KLH-3Mpy1C and BSA-3Mpy1C were purified by size exclusion chromatography using Sephadex G-150 and used for an antigen for the immunization to mice and enzyme-linked immunosorbent assays (ELISA), respectively. The fraction containing protein–porphyrin conjugates was concentrated by ultrafiltration. The concentration of protein was determined by the BCA method. The concentration of porphyrin was determined from the Soret band ($\varepsilon_{421\,nm}=2.3\times10^5\,cm^{-1}\,M^{-1}$). The number of 3Mpy1C on the protein was calculated from molar ratio of 3Mpy1C to the protein. The resulting conjugates contained 180 mol hapten (3MPy1C) per mol KLH and 3.5 mol hapten per mol of BSA. Balb/c mice aged eight weeks were immunized with KLH-3Mpy1C in saline emulsified 1:1 in Freund's complete adjuvant four times at two weeks intervals. Three days after the final injection, the spleen was taken from the mouse and the spleen cells were fused with the SP 2/0 mouse myeloma cells. The hybridomas secreting antibodies for the cationic porphyrin, 3Mpy1C, were detected by ELISA. The hybridomas secreting anti-3Mpy1C antibodies were cloned two times by limiting dilution. Three monoclonal antibodies (34A1F, 12E11G, and 83B5D) specific for 3Mpy1C were obtained and their subclasses were found to be immunoglobulin M (IgM), IgG_1, and IgG_1, respectively. IgG is the most common immunoglogulin with two identical antigen combining sites and the molecular weight of IgG is $\approx$15000. IgM ($M_w=960000$) has a pentameric structure of IgG and ten antigen combining sites in a single molecule. One of these monoclonal antibodies, 12E11G was found to have the highest affinity for 3MPy1C and was used for further experiments.

Bindings of metalloporphyrins to monoclonal antibodies: The binding of monoclonal antibody 12E11G to metalloporphyrins was investigated by ELISA. Monoclonal antibody 12E11G strongly bound to the hapten (3MPy1C) with the dissociation constant of 1.7×10^{-8} M. Figure 1 shows the absorption spectra of the cationic porphyrin, *meso*-tetrakis-(4-*N*-methylpyridyl)porphyrin (TMPyP) in the absence and presence of antibody 12E11G. The Soret band of porphyrin shifted to a longer wavelength (5 nm) and the hypochromism was observed by the addition of antibody 12E11G, indicating that porphyrin is placed in the low-polar environment. Figure 2 shows the circular dichroism spectrum of the porphyrin bound to the antibody. Although TMPyP itself showed no CD peak, the complex showed induced Cotton effects on TMPyP in the region of the Soret band, suggesting that the porphyrin molecule was incorporated into the chiral environment of the combining site of the antibody. The split CD on TMPyP in the presence of the antibody was ascribable to an exciton coupling of the band of porphyrins. This result can be interpreted as indicating that two porphyrin molecules bound to the antibodies were close together. It was suggested that the antibody bound one por-

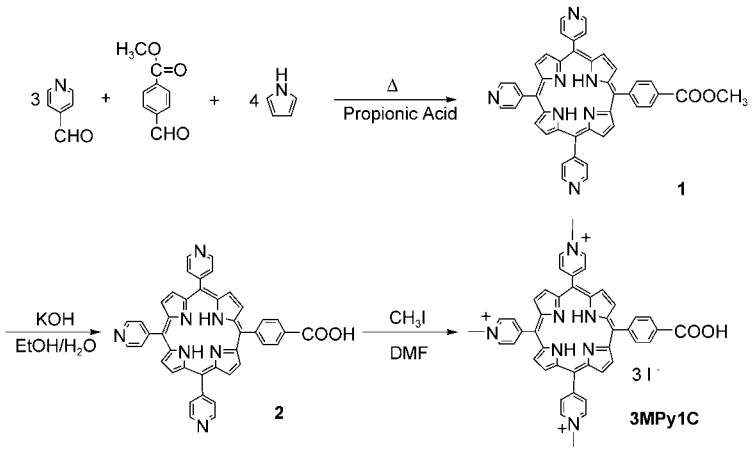

Scheme 1. Preparation of hapten (3MPy1C).

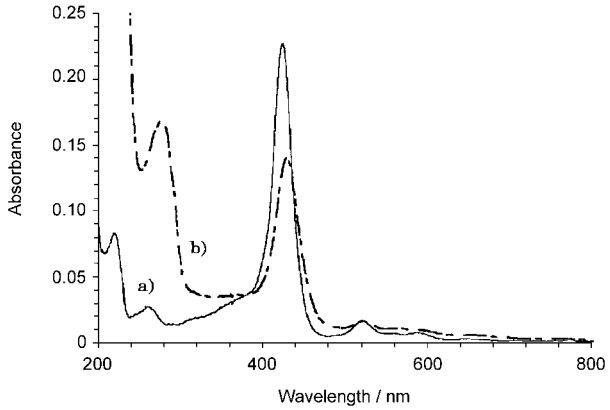

Figure 1. Absorption spectra of TMPyP in a) the absence and b) the presence of anti-3MPy1C antibody (12E11G).

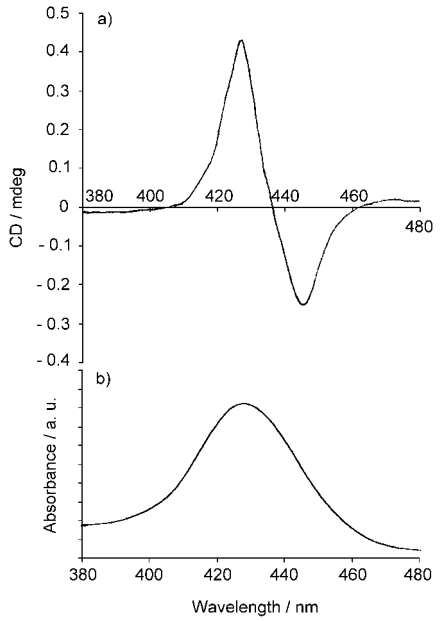

Figure 2. a) CD and b) absorption spectra of TMPyP incorporated in the antibody-combining site.

phyrin molecule and one-to-one complexes of the antibody with the porphyrin associated together to form a two-to-two complex. Similar results were obtained when zinc-tetracarboxyphenylporphyrin was mixed with the anti-porphyrin antibody.[24] Figure 3 shows Klotz plots for the binding of antibody 12E11G to cationic porphyrins bearing the different number of charges in a molecule. The affinity of the antibody to di-cationic porphyrin (*cis*-2MPyP) was lower about

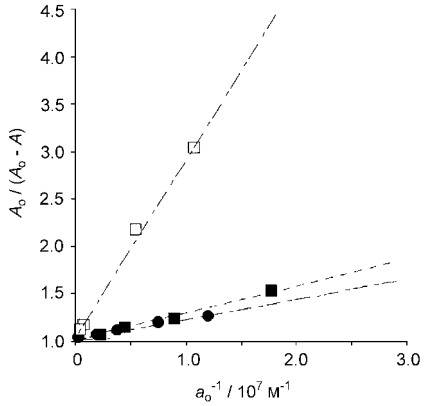

Figure 3. Klotz plots for the binding of antibody 12E11G and cationic porphyrins. Klotz equation is given as follow: $A_0/(A_0-A) = 1+K_d/a_0$, where A_0 and A are absorbances at 405 nm of ELISA in the absence and presence of porphyrins, respectively. K_d is the dissociation constant and a_0 is the total concentration of porphyrins; □: *cis*-2MPyP, ■: TMPyP, ●: 3MPy1C.

one order of magnitude over that to tri- and tetra-cationic porphyrins. It was suggested that more than a half part of porphyrin molecule might be incorporated in the antibody-combining site. Table 1 shows dissociation constants of the complexes between antibody 12E11G and a series of cationic porphyrins. Although the antibody was elicited against free-base porphyrin, the antibody bound not only to TMPyP, but also to Fe^{III}–TMPyP. The dissociation constants of antibody 12E11G with TMPyP and Fe^{III}–TMPyP were 2.1×10^{-8} M and 2.6×10^{-7} M, respectively.

Table 1. Dissociation constants (K_d) of the complexes between antibody 12E11G and water-soluble porphyrins.

Porphyrins	K_d [10^{-8} M]
TMPyP	2.1
3Mpy1C	1.7
cis-2MPyP	15
Fe^{III}–TMPyP	26
TTMAPP	270
TCPP	5100

The binding mode of antibody 12E11G to cationic porphyrins was examined by the study of electron transfer from a series of cationic porphyrins to electron acceptors in the presence of the antibody. When an electron acceptor, 1-naphthalenesulfonate (1-Np) was added to the aqueous solution of TMPyP, the Soret band of TMPyP shifted to a longer wavelength and the fluorescence was quenched by the addition of 1-Np. The spectroscopic change of TMPyP by the addition of 1-Np was ascribable to the photoinduced electron transfer from porphyrin to the electron acceptor, 1-Np. The fluorescence intensity of TMPyP in the presence of an equivalent of antibody 12E11G to TMPyP also decreased by the addition of 1-Np. However, the degree of quenching was a half of that of TMPyP without antibody 1211G. The spectral change in the presence of two-fold equivalent of the antibody to TMPyP was similar to that in a 1:1 mixture of TMPyP with the antibody. Figure 4 shows Stern–Volmer

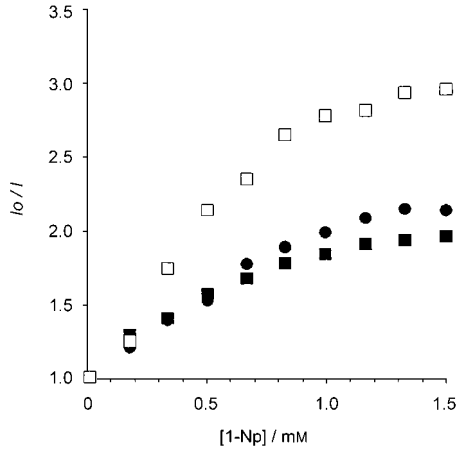

Figure 4. Stern–Volmer plots for the quenching of the emission from Soret band of TMPyP by 1-naphthalenesulfonate (1-Np). [TMPyP]:[antibody binding domain] = 1:0 (□), 1:1 (●), and 1:2 (■).

plots for quenching of the emission from the Soret band of TMPyP by 1-Np in the absence and presence of antibody 12E11G. It was indicated that TMPyP was incorporated in the antibody with stoichiometric 1:1. Figure 5 shows the spectral changes upon titration of *cis*-2MPyP with 1-Np in the absence and presence of antibody 12E11G. When 1-Np was added to an aqueous solution of *cis*-2MPyP, the Soret band of *cis*-2MPyP decreased and shifted toward a longer wavelength, indicating that *cis*-2MPyP has interactions with 1-Np in the ground. This is probably due to the electrostatic interactions between cationic porphyrin and anionic 1-Np. In contrast, when 1-Np was added to an aqueous solution of *cis*-2MPyP in the presence of an equimolar amount of antibody 12E11G, the Soret band did not shift at all and showed no hypochromicity (Figure 5b). Figure 6 shows fluorescence spectral changes of *cis*-2MPyP by the addition of 1-Np in the absence and presence of the antibody. Without antibody, the fluorescence intensity of *cis*-2MPyP decreased as well as TMPyP. However, no fluorescence quenching was observed in the presence of the antibody (Figure 6b); this indicates that there were no interactions between *cis*-2MPyP and

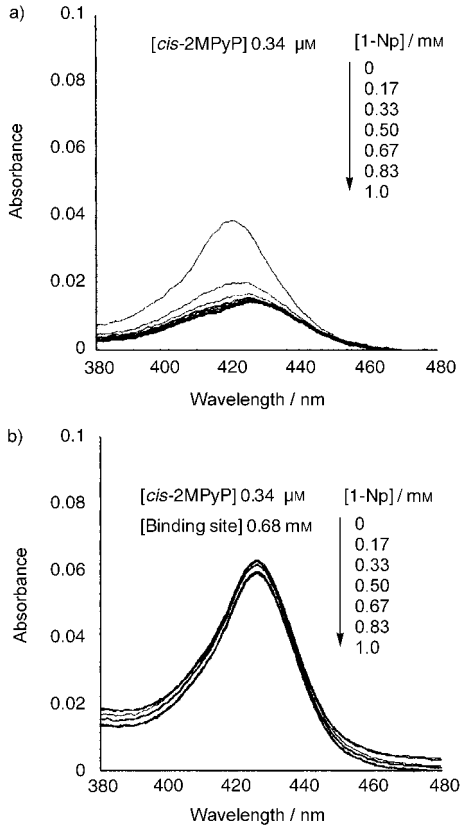

Figure 5. UV/Vis spectra of *cis*-2MPyP in the a) absence and b) presence of antibody 12E11G with 1-Np.

1-Np. No electron transfer from *cis*-2MPyP to 1-Np in the presence of antibody 12E11G suggested that at least two cationic moieties in the *cis*-2MPyP were covered with the binding pocket of the antibody. Figure 7 shows the schematic representation of the complex of *cis*-2MPyP with the antibody. Taking into account dissociation constants of the complexes between the antibody and a series of cationic porphyrins with the results of the photoinduced electron transfer from cationic porphyrins to anionic electron acceptors, more than a half part of porphyrin molecule was incorporated by the antibody-combining site.

Catalytic effects on peroxidation by the antibody- Fe^{III}–TMPyP complex: Catechol, guaiacol, pyrogallol, 2,2′-azinobis(3-ethyl-benzothiazoline-6-sulfonic acid) 2-ammonate (ABTS), and *o*-dianisidine (see below) are known as typical chromogenic substrates to be oxidized by naturally occurring enzyme, horseradish peroxidase (HRP). The catalytic effects of the complex of Fe^{III}–TMPyP with antibody 12E11G on the oxidation of these substrates were investigated. The oxidation reaction was performed under the following conditions. The complex of antibody 12E11G with the cationic iron-porphyrin (0.5 μM) was dissolved in tris-acetate buffer (90 mM, pH 8.0), and incubated for two days at room temperature. Hydrogen peroxide (50 mM) was then added, followed by a substrate. The changes of absorbance at λ_{max} for the oxidation product of each substrate were monitored.[37] Results showed that the Fe^{III}–TMPyP–antibody

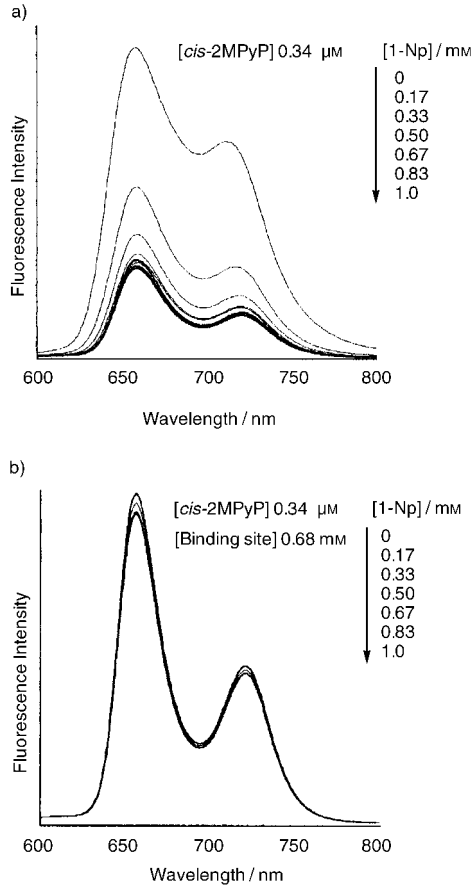

Figure 6. Fluorescence spectral changes of *cis*-2MPyP by the addition of 1-Np: a) absence and b) presence of antibody 12E11G with 1-Np.

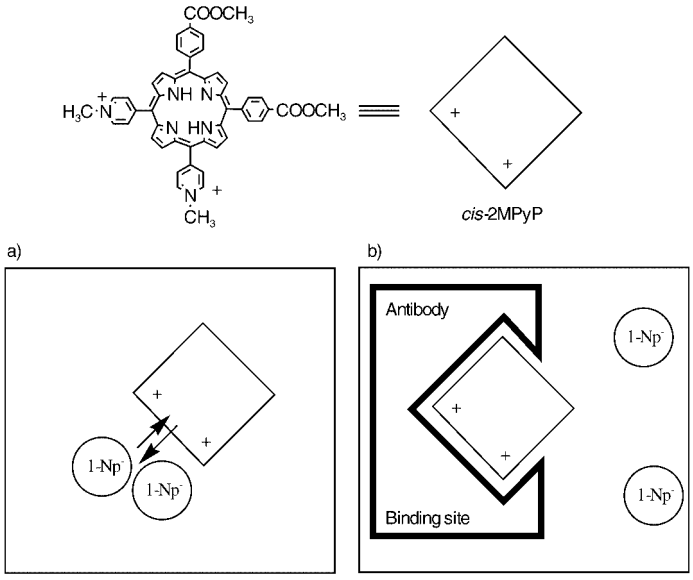

Figure 7. Schematic representation of the complex of the antibody 12E11G with cationic porphyrin (*cis*-2MPyP) and interactions between *cis*-2MPyP and anionic electron acceptor (1-Np) in the a) absence and b) presence of the antibody.

12E11G complex had catalytic effects on catechol, guaiacol, and pyrogallol. Especially, the complex markedly catalyzed the oxidation of pyrogallol. Figure 8 shows the time depend-

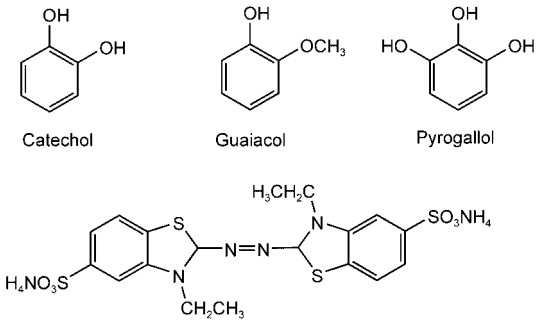

2,2'-Azinobis(3-ethylbenzthiazolin-6-sulfonic acid)diammonium salt (ABTS)

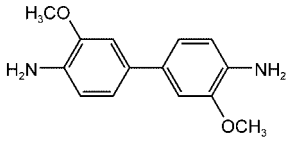

o-Dianisidine

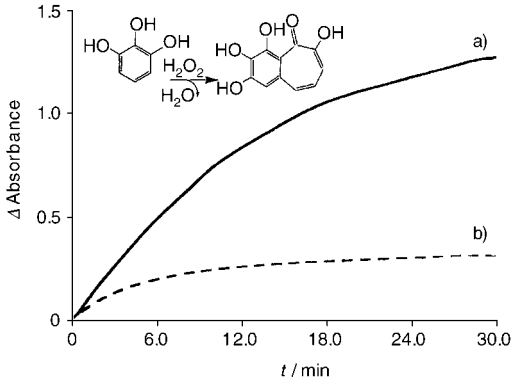

Figure 8. Peroxidation of pyrogallol in a) the presence of the Fe^{III}–TMPyP–antibody 12E11G complex and b) Fe^{III}–TMPyP alone.

ence of oxidation of pyrogallol (1.0 mM) by Fe^{III}–TMPyP in the presence and absence of antibody 12E11G. Peroxidation catalyzed by the antibody–Fe^{III}–TMPyP complex was faster than oxidation in the presence of Fe^{III}–TMPyP alone. Further addition of the substrate caused a further catalytic reaction in the presence of the antibody–Fe^{III}–TMPyP complex, indicating that the catalyst was still active. On the second addition of pyrogallol and hydrogen peroxide to the solution of the complex of the antibody with Fe^{III}–TMPyP, the catalytic oxidation reaction was observed with 80% activity, compared with that on the first addition of these substrates. On the other hand, the catalytic activity of Fe^{III}–TMPyP alone disappeared. It was suggested that the porphyrin catalyst in the absence of the antibody would be destroyed by an excess amount of hydrogen peroxide.

The complex of the antibody with Fe^{III}–TMPyP accelerated the oxidation of smaller substrates such as catechol, guaiacol, and pyrogallol, however, it had no effect on the oxidation of the substrates with a large molecular size such as ABTS or *o*-dianisidine. The substrate specificity of the antibody–Fe^{III}–TMPyP complex on the catalytic oxidation might be due to the limitation of space around the active site by the binding of the antibody to the porphyrin mole-

cule. The complex of Fe^{III}–TMPyP with antibody 83B5D, which was also obtained by the immunization of the 3MPy1C conjugate, had no catalytic effect on the oxidation of pyrogallol and the other substrates. Antibody 12E11G was suggested to have catalytic residues in its antigen combining site and antibody 83B5D was thought to have no binding space for the substrates or no catalytic residues. The clear evidence to explain the difference on the catalytic behavior of these antibody–Fe^{III}–TMPyP complexes may be obtained by comparison of the amino acid sequences of the antigen combining sites in these antibodies. The determination of the nucleotide sequences of the cloned DNA fragments encoding L and H chains of the antibodies, 12E11G and 83B5D, is in progress.

Figure 9a shows a Lineweaver–Burk plot on the oxidation of pyrogallol by the Fe^{III}–TMPyP–antibody complex. The concentration of hydrogen peroxide was fixed and set as the same as that in the previous study.[25] From the plot, the Michaelis constant K_m and the catalytic constant k_{cat} values were calculated. The K_m value in the presence of Fe^{III}–TMPyP–antibody complex was 8.6 mM. The k_{cat} was 680 min^{-1}, which was about eight times as high as that in the absence of the antibody (83 min^{-1}). Previously we reported peroxidase activity of the complex between Fe^{III}–tetracarboxyphenylporphyrin (Fe^{III}–TCPP) and anti-TCPP antibody 03-1 on the oxidation of pyrogallol.[25] The K_m and k_{cat} values of the Fe^{III}–TCPP–antibody 03-1 complex on the oxidation of pyrogallol were 4.0 mM and 50 min^{-1}, respectively. The k_{cat} of the Fe^{III}–TMPyP–antibody 12E11G complex was 13-fold higher than that of the Fe^{III}–TCPP–antibody 03-1 complex. Although the Fe^{III}–TMPyP–antibody 12E11G complex was found to have lower affinity for pyrogallol than the Fe^{III}–TCPP–antibody 03-1 complex by comparison of the K_m, the catalytic activity of the cationic porphyrin–antibody system ($k_{cat}/K_m = 7.9\times10^4$ M^{-1} min^{-1}) was higher than that of the anionic porphyrin–antibody system (1.2×10^4). The increase of the catalytic activity of the Fe^{III}–TMPyP–antibody 12E11G complex was ascribable mainly to the high reactivity of the cationic porphyrin itself and stabilization of Fe-porphyrin by the binding of the antibody.

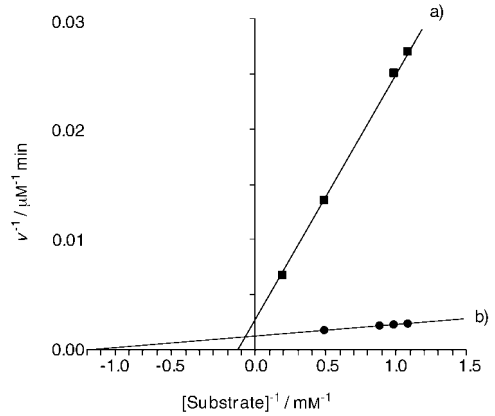

Figure 9. Lineweaver–Burk plots for the oxidation of pyrogallol as a function of substrate (pyrogallol) in the presence of a) the complex of antibody 12E11G with Fe^{III}–TMPyP and b) HRP.

Comparison of catalytic activities of metalloporphyrin–antibody complexes with those of native peroxidase: Figure 9b shows a Lineweaver–Burk plot in the oxidation of pyrogallol in the presence of HRP with 50 mM H_2O_2. From the plot, the K_m and k_{cat} values for HRP were estimated to be 0.8 mM and 1750 min^{-1}, respectively. The k_{cat} of HRP was three times as high as that of the Fe^{III}–TMPyP–antibody complex. Although the k_{cat}/K_m value was 2.2×10^6 M^{-1} min^{-1} for HRP, being 28 times higher than that of the Fe^{III}–TMPyP–antibody complex, the Fe^{III}–TMPyP–antibody complex was highly reactive (Table 2). The catalytic activity of HRP decreased at higher concentrations of H_2O_2, however, that of the antibody–porphyrin complex was retained.

Table 2. Kinetic parameters for the oxidation of pyrogallol.

Catalysts	K_m [mM]	k_{cat} [min^{-1}]	k_{cat}/K_m [M^{-1} min^{-1}]
Fe^{III}–TMPyP		83	
Fe^{III}–TMPyP–Ab·12E11G	8.6	680	7.9×10^4
Fe^{III}–TCPP[a]		8.7	
Fe^{III}-TCPP-Ab·03-1[b]	4.0	50	1.2×10^4
HRP	0.81	1750	2.2×10^6

[a] Tetrakis-*meso*-(4-carboxyphenyl)porphyrin iron complex. [b] Monoclonal antibody elicited against TCPP.

The naturally occurring enzyme, HRP, catalyzes the oxidations of various substrates, not only pyrogallol but also hydroquinone, catechol, resorcinol, guaiacol, ABTS, and *o*-dianisidine. The reactions promoted by HRP are nonspecific. By contrast, the catalytic oxidation by the Fe^{III}–TMPyP–antibody complex was selective for small molecular substrates such as catechol, guaiacol, and pyrogallol.

Conclusion

We have obtained monoclonal antibodies for a cationic porphyrin. One of the antibodies, 12E11G, bound the cationic porphyrin selectively and formed stable complexes with the porphyrins and metalloporphyrins. The complex of antibody 12E11G with Fe^{III}–TMPyP was found to have catalytic activity for the oxidation of catechol, guaiacol, and pyrogallol. The metalloporphyrin–antibody complex was stable enough to show catalytic activity in the presence of an excess amount of H_2O_2. The catalytic activity of the cationic porphyrin-antibody complex for the oxidation of pyrogallol was higher than that of the anionic porphyrin–antibody complex and active as a catalyst even under the conditions which porphyrin alone or HRP should lose their catalytic activity.

Experimental Section

Materials: HRP was purchased from Wako Pure Chemical Industries. Myeloma cell (Sp2/0-Ag14) and goat-anti-mouse immunoglobulin were obtained from Dainippon Pharmaceutical Co. and CAPPEL, respectively. Other chemicals were purchased from Nacalai Tesque Inc. or Sigma-Aldrich and used without further purification. All solvents were of technical grade.

[5-(Methoxycarboxyphenyl)-10,15,20-tris-(4-pyridyl)]porphine (1): Isonicotine-aldehyde (23.2 g, 0.22 mol) and terephthalaldehydic acid methyl ester (11.9 g, 0.073 mol) were added to propionic acid (2.0 L).[38] The mixture refluxed in a 3-neck flask under nitrogen atmosphere. Subsequently pyrrole (20 mL) was added dropwise to the refluxing mixture within 30 min. The reaction mixture was heated under reflux for another 90 min and then allowed to cool to room temperature. Almost all the propionic acid was evaporated from the mixture. Porphyrin **1** was purified by silica gel column chromatography by using 3% MeOH in $CHCl_3$ as eluent. Yield: 12.4 mg from 1.0 g reaction mixture, 1.4%. ^{1}H NMR ($CDCl_3$): $\delta =$ 9.1 (d, 6H), 8.9 (m, 8H), 8.5 (d, 4H), 8.2 (d, 6H), 4.1 (s, 3H), −2.9 (s, 2H); elemental analysis calcd (%) for $C_{43}H_{29}N_7O_2 \cdot 0.17\,CHCl_3$: C 74.47, H 4.22, N 14.08; found: C 74.47, H 4.32, N 13.98.

[5-(Carboxyphenyl)-10,15,20-tris-(4-pyridyl)]porphine (2): Tri-pyridyl porphyrin **1** was dissolved in 2 M KOH in 80% EtOH and stirred at room temperature for 3 d. The product was extracted by $CHCl_3$ and dried over anhydrous $NaSO_4$. The solvent was removed by a rotary evaporator. The residue was dried under vacuum. ^{1}H NMR ($CDCl_3$/CD_3OD): $\delta =$8.2 (d, 6H), 8.9 (d, 8H), 7.5 (d, 4H), 7.4 (d, 6H), −3.8 (s, 2H).

[5-(4-Carboxyphenyl)-10,15,20-tris-(4-methylpyridyl)]porphine iodide (3MPy1C): Porphyrin **2** (19.5 mg, 18 mmol) was dissolved in DMF (3 mL). Subsequently CH_3I (3 mL, 48 mmol) was added to the solution and the mixture was heated under reflux for 2 h.[39] The solution was poured into acetone (50 mL). The resulting precipitate was washed with $CHCl_3$ and dried under vacuum. Yield: 27 mg, 84.3%. ^{1}H NMR ([D_6]DMSO): $\delta =$13.4 (s, 1H), 9.5 (d, 6H), 9.2 (m, 14H), 8.4 (d, 4H), 4.7 (s, 9H), −3.0 (s, 2H); UV/Vis (λ_{max}) = 645, 587, 560, 520, 423, 259, 224 nm in pH 9.0 phosphate borate buffer (PBB, 0.1 M); elemental analysis calcd (%) for $C_{45}H_{36}N_7O_2I_3 \cdot 4H_2O$: C 46.58, H 3.82, N 8.45; found: C 46.58, H 3.75, N 8.24.

Hapten-carrier protein conjugates: Hapten 3MPy1C (8.3 mg, 7.6 mmol) and carbonyldiimidazole (1.5 mg, 9.3 mmol) were dissolved in DMF (2.0 mL) and stirred at 4°C for 2 h. Subsequently the solution was added dropwise to PBB (pH 9.0, 8.0 mL) containing keyhole limpets hemocyanin (KLH, 5.0 mg) with stirring at 4°C overnight. The product was purified by column chromatography on Sephadex G-150 with PBB as eluent. The absorbances at 280 nm and Soret band of porphyrins ($\varepsilon_{421\,nm} = 2.3 \times 10^5\,M^{-1}cm^{-1}$) were monitored for each fraction.

Preparation of monoclonal antibodies: The conjugate of 3MPy1C with KLH dissolved in phosphate buffered saline (PBS) was emulsified in Freund's complete adjuvant. Balb/c mice (7–8 weeks old) were immunized with the 3MPy1C–KLH conjugate (60 μg). Immunizations were done at intervals of 2 weeks until the mice showing the best immune response. At boost, the mouse was immunized with 3MPy1C-KLH (150 μg) without the adjuvant.

Myeloma cells were cultured in 10% FBS RPMI 1640 medium. The three days after the last injection of immunogen, the spleen was removed from an immunized mouse. The spleen cells were washed with a hemolysis buffer and medium by centrifugation. The spleen cells and myeloma cells were mixed and centrifuged. The cell pellet was mixed by tapping the tube, added PEG solution to prepare the fused cells, and incubated at 37 C. After the addition of PEG solution, the medium (2.0 mL) was added to the cell suspension. Cells were collected by centrifugation and removed supernatant. Cell pellet was suspended in 10% FBS medium with hypoxanthines, aminopterin, and thymidine (HAT). They were plated in ten 96-well plates with peritoneal macrophages as a feeder layer.

The initial screen for antibody activity was carried out as when the growth of hybrid cells was seen under the microscope or when the pH indicator dyes in medium became yellow. The antibodies produced by cells were assayed by ELISA for 3MPy1C binding. The tissue culture supernatants were added onto the ELISA plate coated with 0.3 mg mL^{-1} BSA-3Mpy1C and incubated at 37°C for 90 min. The amount of antibody bound to the antigen was measured using goat anti-mouse immunoglobulins labeled antibody with alkaline phosphatase. Positive wells were cloned in 10% FBS HT medium. The positive cells were diluted at about 2–3 cells mL^{-1} and plated in 96 well plates with macrophage feeder layers. The plate that 60% of the wells received only one clone was selected and screened by ELISA.

Hybridoma cells were injected to mice. After 10–14 d, the ascitic fluid was drained off through 18G needle. The ascitic fluid was centrifuged and the supernatant was stored at −20°C. Antibodies were purified by affinity chromatography using Ampure PA kit (Amersham) for IgG.

Isotypes of antibodies: The hybridoma supernatant (0.5 mL) in tris(hydroxymethyl)aminomethane/HCl buffer containing 1% Tween 20 (TBS-T, 4.5 mL) was added to the typing stick (Sigma) in the container. After 15 min incubation at room temperature, the stick was washed with TBS-T. After washing, a peroxidase labeled anti-mouse antibody in TBS-T (3.0 mL) was added to the container and incubated for 15 minutes at room temperature. A substrate solution (hydrogen peroxide and 4-chloro-1-naphthol) was added to the container. After 15 minutes incubation at room temperature, the stick was washed with water and the oxidation product by the enzymatic reaction was monitored as a color change.

[5,10-Bis(4-carboxyphenyl)-15,20-bis-(4-methylpyridyl)]porphine methyl ester (*cis*-2MPyP): *cis*-2MPyP was prepared by methylation of [5,10-bis(4-methoxy-carboxyphenyl)-15,20-bis-(4-pyridyl)]porphine, formed during the synthesis of porphyrin **1**, and separated by the same way as for **1**. ^{1}H NMR ([D_6]DMSO)/: $\delta =$9.4 (d, 4H), 9.1 (s, 2H), 9.0 (m, 8H), 8.9 (s, 2H), 8.4 (d, 8H), 4.7 (s, 6H), 4.0 (s, 6H), −3.0 (s, 2H); elemental analysis calcd (%) for $C_{47}H_{38}N_6I_2O_4 \cdot 3.3\,H_2O$: C 53.05, H 4.22, N 7.90; found: C 53.01, H 4.10, N 7.70.

[5,10,15,20-Tris-(4-methylpyridyl)]porphine iron(III) chloride (Fe^{III}-TMPyP): The insertion of iron to the porphyrin center was carried out by adding solid $FeCl_2$ to a refluxing aqueous solution of TMPyP under a nitrogen atmosphere. TMPyP (250 mg) was dissolved in water (100 mL), and the solution was refluxed for 2 h with 500-fold excess of $FeCl_2 \cdot 4H_2O$. The solution was then cooled at room temperature and added excess sodium perchlorate solution to the precipitate. The reaction mixture was allowed to stand overnight, filtered, and washed 6–7 times with 2.0% perchloric acid to remove excess metal ions. The resulting paste was dried under vacuum and then dissolved in CH_3CN. Tetraethylammonium chloride was added to the solution to the precipitate. The metalloporphyrin, Fe^{III}–TMPyP(Cl_5), was dried under vacuum. UV/Vis (water): $\lambda_{max} =$632, 596, 421 nm; elemental analysis calcd (%) for $FeC_{44}H_{38}N_8Cl_5 \cdot 12.5\,H_2O$: C 46.47, H 5.58, N 9.85; found C 46.47, H 5.36, N 10.08.

Measurements: Absorbance at 405 nm for the product of the enzymatic reaction on the ELISA was recorded on a Immuno-Mini NJ-2300. UV/Vis spectra were recorded on a Shimadzu UV-2500PC. Proton NMR spectra were recorded on a JEOL JNM-GX 270. Chemical sifts are given in ppm relative to $CDCl_3$ or [D_6]DMSO. Circular dichroism spectra were recorded on a JASCO J-40A spectrophotometer with a JASCO ORD/CD data processor using a 10 mm quartz cell. Emission spectra were recorded with a Hitachi F-2500 fluorescence spectrophotometer.

Binding properties of antibodies: A competitive inhibition immunoassay based on ELISA was used for determination of dissociation constants between antibodies and porphyrins.[40] Plates are treated with blocking buffer for 90 minutes at 37°C to prevent antibodies from nonspecific binding to the surface of the plate. Solutions of various porphyrins (10^{-5}–10^{-9} M) were prepared. The antibody solution (60 μL) and porphyrin solutions (60 μL) were added to the blocked plate, and incubated for 2 h at room temperature. Subsequently, 100 μL of each reaction mixture was added to the other plate that coated by 3MPy1C-BSA, and the remained antibodies were assayed by ELISA.

The electron transfer from TMPyP or *cis*-2MPyP to 1-naphthalenesulfonate (1-Np) in the absence and presence of the antibody was evaluated by the Stern-Volmer plots. Rate constants of electron transfer were determined by the Stern–Volmer Equation (1) given by

$$\frac{I_o}{I} = 1 + K_{SV}[Q] \qquad (1)$$

where I_o and I are fluorescence intensities in the absence and presence of the quencher, respectively. K_{SV} is the Stern–Volmer constant and [Q] the concentration of the quencher. All measurements were carried out in 1.25 mM tetrasodium ethylenediaminetetraacetate (EDTA-4Na) and 100 mM phosphate borate buffer (PBB, pH 9.0). A solution of 1-Np (0–1.5 mM) was added to the solution of porphyrin in the absence and presence of antibody 12E11G. The ratios of the concentration of porphyrin to

that of antibody combining site were fixed at 1:0, 1:1, and 1:2, respectively. The final concentration of porphyrin was 0.34 μM.

Peroxidase activity: Kinetic study was performed under the following conditions. Horseradish peroxidase or the complex of antibody 12E11G with cationic metalloporphyrin was dissolved in tris-acetate buffer (90 mM, pH 8.0), and incubated for 2 days at room temperature. Hydrogen peroxide was then added, followed by a substrate. The starting time was set at this point. The changes of absorbance for the oxidation product of were monitored.[25,41–43] Reaction mixtures contained 50 mM hydrogen peroxide, 0.5 μM metalloporphyrin, 0.8 μM antibody, 4% *v/v* DMSO, and 90 mM tris-acetate (pH 8.0).

Acknowledgement

The authors thank Dr. L. Brunsveld, Laboratory of Macromolecular and Organic Chemistry, Eindhoven University of Technology (The Netherlands) for collaboration of the preparation of cationic porphyrin derivatives and Prof. T. Sato, Graduate School of Science, Osaka University, for the CD measurements. The authors express their special thanks for the center of excellence (21COE) program "Creation of Integrated Eco-Chemistry" of Osaka University.

[1] D. Dolphin, *The Porphyrins*, Academic Press, New York, **1978**.
[2] K. M. Kadish, K. M. Smith, R. Guilard, *The Porphyrin Handbook*, Academic Press, San Diego, **1999**.
[3] C. J. Reedy, B. R. Gibney, *Chem. Rev.* **2004**, *104*, 617–649.
[4] A. Lombardi, F. Nastri, V. Pavone, *Chem. Rev.* **2001**, *101*, 3165–3189.
[5] D. A. Mofft, M. H. Hecht, *Chem. Rev.* **2001**, *101*, 3191–3204.
[6] H. K. Rau, W. Haehnel, *J. Am. Chem. Soc.* **1998**, *120*, 468–576.
[7] M. Takahashi, A. Ueno, H. Mihara, *Chem. Eur. J.* **2000**, *6*, 3196–3203.
[8] D. A. Moffet, L. K. Certain, A. J. Smith, A. J. Kessel, K. A. Beckwith, M. H. Hecht, *J. Am. Chem. Soc.* **2000**, *122*, 7612–7613.
[9] K. Y. Tomizaki, H. Nishino, T. Arai, T. Kato, N. Nishino, *Chem. Lett.* **2003**, *32*, 6–7.
[10] Y. Lu, S. M. Berry, S. T. D. Plister, *Chem. Rev.* **2001**, *101*, 3047–3080.
[11] Y. Watanabe, *Curr. Opin. Chem. Biol.* **2002**, *6*, 208–216.
[12] T. Hayashi, T. Takimura, H. Ogoshi, *J. Am. Chem. Soc.* **1995**, *117*, 11606–11607.
[13] I. Hamachi, S. Tanaka, S. Tsukiji, S. Shinkai, M. Shimizu, T. Nagamune, *Chem. Commun.* **1997**, 1735–1736.
[14] Y. Z. Hu, S. Tsukiji, S. Shinkai, S. Oishi, I. Hamachi, *J. Am. Chem. Soc.* **2000**, *122*, 241–253.
[15] T. Hayashi, Y. Hisaeda, *Acc. Chem. Res.* **2002**, *35*, 35–43.
[16] S. J. Pollack, G. R. Nakayama, P. G. Schultz, *Science* **1988**, *242*, 1038–1042.
[17] S. J. Pollack, P. G. Schultz, *J. Am. Chem. Soc.* **1989**, *111*, 1929–1931.
[18] A. W. Schwabacher, M. I. Weinhouse, M.-T. M. Auditor, R. A. Lerner, *J. Am. Chem. Soc.* **1989**, *111*, 2344–2346.
[19] A. Harada, K. Okamoto, M. Kamachi, T. Honda, T. Miwatani, *Chem. Lett.* **1990**, 917–918.
[20] A. G. Cochran, P. G. Schultz, *J. Am. Chem. Soc.* **1990**, *112*, 9414–9415.
[21] A. G. Cochran, P. G. Schultz, *Science* **1990**, *249*, 781–783.
[22] A. Harada, K. Okamoto, M. Kamachi, *Chem. Lett.* **1991**, 953–956.
[23] E. Keinan, E. Benory, S. C. Sinha, A. Sinha-Bagchi, D. Eren, Z. Eshhar, B. S. Green, *Inorg. Chem.* **1992**, *31*, 5433–5438.
[24] A. Harada, K. Shiotsuki, H. Fukushima, H. Yamaguchi, M. Kamachi, *Inorg. Chem.* **1995**, *34*, 1070–1076.
[25] A. Harada, H. Fukushima, K. Shiotsuki, H. Yamaguchi, F. Oka, M. Kamachi, *Inorg. Chem.* **1997**, *36*, 6099–6102.
[26] A. D. Wentworth, L. H. Jones, P. J. Wentworth, K. D. Janda, R. A. Lerner, *Proc. Natl. Acad. Sci. USA* **2000**, *97*, 10930–10935.
[27] P. J. Wentworth, L. H. Jones, A. D. Wentworth, X. Zhu, N. A. Larsen, I. A. Wilson, X. Xu, W. A. Goddard, K. D. Janda, A. Eschenmoser, R. A. Lerner, *Science* **2001**, *293*, 1806–1811.
[28] J. K. M. Sanders, *Chem. Eur. J.* **1998**, *4*, 1378–1383.
[29] H. Yamaguchi, M. Kamachi, A. Harada, *Angew. Chem.* **2000**, *112*, 3987–3989; *Angew. Chem. Int. Ed.* **2000**, *39*, 3829–3831.
[30] M. C. Feiters, A. E. Rowan, J. M. Nolte, *Chem. Soc. Rev.* **2000**, *29*, 375–384.
[31] R. Ricoux, H. Sauriat-Dorizon, E. Girgenti, D. Blanchard, J.-P. Mahy, *J. Immunol. Methods* **2002**, *269*, 39–57.
[32] B. Ward, A. Skorobogaty, J. C. Dabrowiak, *Biochemistry* **1986**, *25*, 6875–6883.
[33] R. F. Pasternack, B. Halliwell, *J. Am. Chem. Soc.* **1979**, *101*, 1026–1031.
[34] R. F. Pasternack, E. J. Gibbs, J. J. Villafranca, *Biochemistry* **1983**, *22*, 2406–2414.
[35] B. Ward, A. Skorobogaty, J. C. Dabrowiak, *Biochemistry* **1986**, *25*, 7827–7833.
[36] T. Ohse, S. Nagaoka, Y. Arakawa, H. Kawakami, K. Nakamura, *J. Inorg. Biochem.* **2001**, *85*, 201–208.
[37] Peroxidations of pyrogallol, catechol, guaiacol, *o*-dianisidine, and ABTS were monitored at 420 nm, 387 nm, 470, 500, and 414 nm, respectively.
[38] R. G. Little, J. A. Anton, P. A. Loach, J. A. Ibers, *J. Heterocycl. Chem.* **1975**, *12*, 343–349.
[39] M. Perree-Fauvet, C. Verchere-Beaur, E. Tarnaud, G. Anneheim-Herbelin, N. Bone, A. Gaudemer, *Tetrahedron* **1996**, *52*, 13569–13588.
[40] B. Friguet, A. F. Chaffotte, L. Djavadi-Ohaniance, M. E. Goldberg, *J. Immunol. Methods* **1985**, *77*, 305–310.
[41] A. P. Savitsky, M. I. Nelen, A. K. Yatsmirsky, M. V. Demcheva, G. V. Ponomarev, I. V. Sinikov, *Appl. Biochem. Biotechnol.* **1994**, *47*, 319–327.
[42] Y. Feng, Z. Liu, S. J. Gao, X. Y. Liu, T. S. Yang, *Ann. N. Y. Acad. Sci.* **1995**, *750*, 271–276.
[43] S. de Lauzon, D. Mansuy, J. -P. Mahy, *Eur. J. Biochem.* **2002**, *269*, 470–480.

Received: November 6, 2003
Revised: August 18, 2004
Published online: October 29, 2004

